

Subcarrier Combining for Analog SC-FDE

Thanh Hai VO[†] Shinya KUMAGAI[†] and Fumiyuki ADACHI[‡]

[†] [‡] Department of Communications Engineering, Graduate School of Engineering, Tohoku University

6-6-05 Aza-Aoba, Aramaki, Aoba-ku, Sendai-shi, Miyagi, 980-8579 Japan

E-mail: [†] {vothanhai, kumagai}@mobile.ecei.tohoku.ac.jp, [‡] adachi@ecei.tohoku.ac.jp

Abstract Recently, we proposed analog single-carrier transmission with frequency-domain equalization (analog SC-FDE) in order to improve performance of analog signal transmission. Analog SC-FDE signal spectrum has a complex conjugate relation between lower sideband (LSB) and upper sideband (USB) since analog signal is real-valued. Exploiting this property, the LSB and USB subcarriers can be combined to obtain an additional frequency diversity gain. In this paper, a subcarrier combining method is proposed for analog SC-FDE. A theoretical analysis of normalized mean square error (NMSE) performance is also presented to evaluate the effect of subcarrier combining and is confirmed by computer simulation. We show that subcarrier combining achieves similar diversity order to 2-branch antenna diversity. In addition, the impact of channel frequency-selectivity on the NMSE performance was also investigated to show the effectiveness of proposed scheme.

Keyword Analog SC-FDE, Subcarrier combining, Antenna diversity

1. Introduction

Digital wireless signal transmission technology has been continuously evolving and is widely adopted in most of wireless communication systems [1]-[2]. However, analog signal transmission is still attractive from the view of spectrum efficiency. The signal bandwidth of analog signal transmission is much narrower than that of digital signal transmission because neither source coding nor channel coding is used. Due to the narrowband nature, the propagation channel in the analog signal transmission is considered to be frequency-nonselective [3]. Consequently, the received signal suffers from frequent fades and its quality degrades severely when either a transmitter or a receiver moves during communication. In order to overcome this problem, we recently proposed an analog single-carrier transmission with frequency-domain equalization (analog SC-FDE) [4].

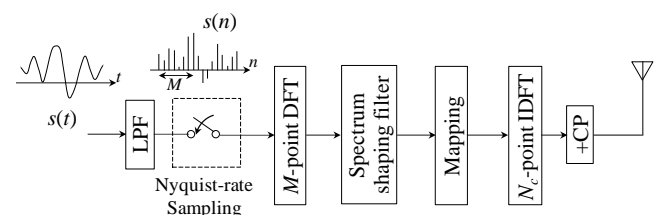
Analog SC-FDE applies discrete Fourier transform (DFT), frequency-domain spectrum shaping and mapping, inverse DFT (IDFT), and cyclic prefix (CP) insertion before transmission. At the receiver, one-tap FDE [5]-[6] is applied to take advantage of frequency-selective fading channel. Multi-access using analog SC-FDE is possible based on the principle of frequency-division multiple access (FDMA). Therefore, the spectrum efficiency is the same as conventional analog signal transmission, inherently narrowband. We showed in [4] that analog SC-FDE achieves better normalized mean square error (NMSE) performance than the conventional analog signal transmission. In particular, combination of distributed mapping [7] and minimum mean square error (MMSE)-based equalization gives the best performance.

In analog SC-FDE, since the analog signal is real-valued, the frequency components of upper sideband (USB) and lower sideband (LSB) spectrum have a complex conjugate relation. Therefore, the corresponding received subcarriers, which have complex conjugate relation in the desired signals, can be combined to obtain an additional frequency diversity gain. In this paper, we propose a subcarrier combining method for analog SC-FDE in order to further improve the NMSE performance. A theoretical analysis of the NMSE performance is also presented and is confirmed by computer simulation.

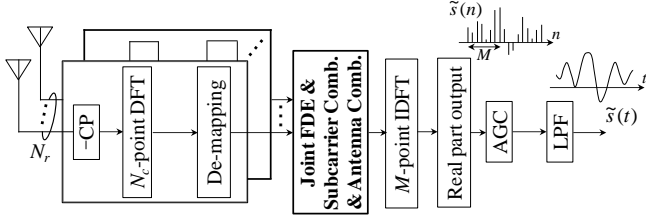
The remainder of this paper is organized as follows. In Section 2, the subcarrier combining method is proposed for analog SC-FDE. The theoretical analysis of NMSE performance is given in Section 3. Section 4 provides the numerical and computer simulation results. Finally, conclusion is presented in Section 5.

2. Subcarrier Combining for Analog SC-FDE

The transmission system model of analog SC-FDE with subcarrier combining is illustrated in Fig. 1. In this paper, we consider a system with single transmit antenna and N_r receive antennas.



(a) Transmitter



(b) Receiver

Fig. 1. System model.

2.1. Transmit Signal Representation

At the transmitter, after limiting bandwidth by low-pass filter (LPF), the analog signal $s(t)$ is sampled at the Nyquist rate of $1/T$. The sample sequence is then grouped into a sequence of signal blocks of M samples each. Each signal block $\{s(n); n=0 \sim M-1\}$ is directly transformed by M -point DFT into frequency-domain signal block $\{S(k); k=0 \sim M-1\}$ without quantization and source encoding. The k -th frequency component $S(k)$, $k=1 \sim M/2-1$, of LSB can be expressed as

$$S(k) = \frac{1}{\sqrt{M}} \sum_{n=0}^{M-1} s(n) \exp\left(-j2\pi k \frac{n}{M}\right) \quad (1)$$

$$= \left[\frac{1}{\sqrt{M}} \sum_{n=0}^{M-1} s(n) \exp\left(-j2\pi(M-k) \frac{n}{M}\right) \right]^* = S^*(M-k)$$

From Eq. (1), it is obvious that there is a complex conjugate relation between the frequency components of LSB $\{S(k); k=1 \sim M/2-1\}$ and USB $\{S(k); k= M/2+1 \sim M-1\}$ except $S(0)$ and $S(M/2)$ as shown in Fig. 2.

The spectrum shaping filter is assumed as an ideal brick wall LPF to transmit the whole spectrum of analog signal. After that, the mapping operation assigns the M resultant frequency components over a broader bandwidth having N_c ($\gg M$) orthogonal subcarriers to take advantage of channel frequency-selectivity (i.e., frequency diversity). The mapping is performed in accordance with distributed mode [7], where the frequency components $\{S(k); k=0 \sim M-1\}$ are mapped uniformly over the bandwidth having N_c subcarriers $\{X(k'); k'=0 \sim N_c-1\}$ as

$$X(k') = \begin{cases} S(k) & , k' = k \times \frac{N_c}{M} \\ 0 & , \text{otherwise} \end{cases} \quad (2)$$

The unused subcarriers, which are occupied by zeros, are assigned to other users. An example of distributed mapping with $M=8$, $N_c=32$ is illustrated in Fig. 3.

The resultant frequency-domain signal having N_c subcarriers is transformed by N_c -point IDFT back into time-domain. A signal block $\{x(n); n=0 \sim N_c-1\}$ at a rate of $1/T_s = (N_c/M) \times 1/T$ is obtained as

$$x(n) = \frac{1}{N_c} \sum_{k=0}^{N_c-1} X(k) \exp\left(j2\pi n \frac{k}{N_c}\right) \quad (3)$$

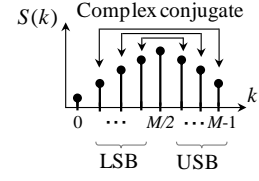


Fig. 2. The spectrum of analog SC-FDE signal.

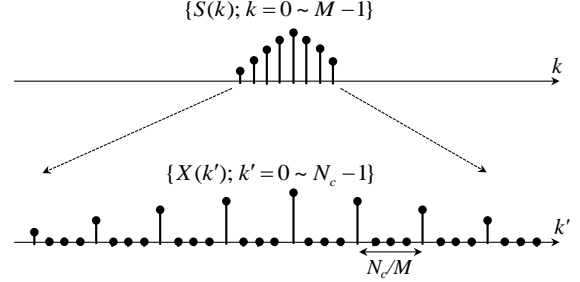


Fig. 3. Distributed mapping.

The discrete-time signal blocks $\{\tilde{x}(n); n=-N_g \sim N_c-1\}$ after inserting CP can be expressed using the equivalent low-pass representation as

$$\tilde{x}(n) = \sqrt{2P} x(n \bmod N_c), \quad (4)$$

where P is the average transmit power.

2.2. Received Signal Representation

A quasi-static frequency-selective channel consisting of L distinct propagation paths is assumed, where the channel stays constant during the signal transmission period of one block. The maximum time delay of channel is considered to be shorter than the CP length. The channel impulse response $h_{n_r}(\tau)$, $n_r=0 \sim N_r-1$, can be expressed as

$$h_{n_r}(\tau) = \sum_{l=0}^{L-1} h_{n_r,l} \delta(\tau - \tau_{n_r,l}), \quad (5)$$

where $h_{n_r,l}$, $\tau_{n_r,l}$, and $\delta(\cdot)$ are the complex-valued path gain with $E[\sum_{l=0}^{L-1} |h_{n_r,l}|^2] = 1$ ($E[\cdot]$ denotes the ensemble average operation), sample-spaced time delay of the l -th path (i.e., $\tau_{n_r,l} = l$), and delta function, respectively.

The transmitted signals are received by N_r receive antennas. It is assumed that the received signal is ideally sampled at the rate $1/T_s$. The discrete-time received signal $\{r_{n_r}(n); n=-N_g \sim N_c-1\}$ at the n_r -th receive antenna is described as

$$r_{n_r}(n) = \sum_{l=0}^{L-1} h_{n_r,l} \tilde{x}(n - \tau_{n_r,l}) + z_{n_r}(n), \quad (6)$$

where $z_{n_r}(n)$ is the complex Gaussian noise sample with zero-mean and variance $2N_0/T_s$ with N_0 being the single-sided power spectrum density of the additive white Gaussian noise (AWGN). After removing CP, each received signal block is decomposed by N_c -point DFT into N_c orthogonal subcarriers $\{R_{n_r}(k); k=0 \sim N_c-1\}$. $R_{n_r}(k)$ is expressed as

$$R_{n_r}(k) = \sqrt{2P} H_{n_r}(k) X(k) + Z_{n_r}(k), \quad (7)$$

where $H_{n_r}(k)$ and $Z_{n_r}(k)$ are respectively the channel gain and the noise component given by

$$\begin{cases} H_{n_r}(k) = \sum_{l=0}^{L-1} h_{n_r,l} \exp\left(-j2\pi k \frac{\tau_{n_r,l}}{N_c}\right) \\ Z_{n_r}(k) = \frac{1}{\sqrt{N_c}} \sum_{n=0}^{N_c-1} z_{n_r}(n) \exp\left(-j2\pi k \frac{n}{N_c}\right) \end{cases} \quad (8)$$

The de-mapping is the reverse operation of the mapping done at the transmitter in order to pick out the desired subcarriers $\{\hat{R}_{n_r}(k); k=0 \sim M-1\}$ and the corresponding channel gain $\{\hat{H}_{n_r}(k); k=0 \sim M-1\}$ as

$$\begin{cases} \hat{R}_{n_r}(k) = R_{n_r}(k \times N_c / M) \\ \hat{H}_{n_r}(k) = H_{n_r}(k \times N_c / M) \end{cases} \quad (9)$$

2.3. Joint Subcarrier Combining and FDE with Receive Antenna Diversity

By exploiting the complex conjugate relation in desired signal between LSB and USB subcarriers, joint subcarrier combining and FDE can be performed to demodulate the frequency components $\{\tilde{S}(k); k=0 \sim M-1\}$ of recovered analog signal. In addition, antenna combining is also carried out to obtain space diversity gain as shown in Fig. 4. The k -th demodulated frequency component $\tilde{S}(k)$ is expressed as

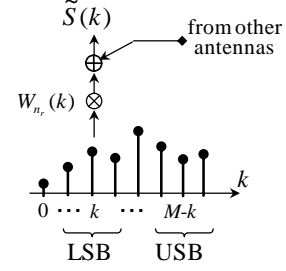
$$\tilde{S}(k) = \begin{cases} \sum_{n_r=0}^{N_r-1} W_{n_r}(k) \hat{R}_{n_r}(k) & , k=0, M/2 \\ \sum_{n_r=0}^{N_r-1} \{W_{n_r,1}(k) \hat{R}_{n_r}(k) + W_{n_r,2}(M-k) \hat{R}_{n_r}^*(M-k)\} & , \text{otherwise} \end{cases} \quad (10)$$

where $W_{n_r}(k)$, $W_{n_r,1}(k)$, and $W_{n_r,2}(k)$ are MMSE-FDE weights designed to minimize mean square error (MSE) between the demodulated signal $\tilde{S}(k)$ and transmitted signal $\sqrt{2PS}(k)$. They are described as [6]

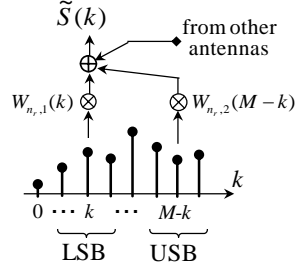
$$W_{n_r}(k) = \frac{\hat{H}_{n_r}^*(k)}{\sum_{n_r=0}^{N_r-1} |\hat{H}_{n_r}(k)|^2 + \Gamma^{-1}}, \quad \text{for } k=0, M/2 \quad (11)$$

$$\begin{cases} W_{n_r,1}(k) = \frac{\hat{H}_{n_r}^*(k)}{\sum_{n_r=0}^{N_r-1} (|\hat{H}_{n_r}(k)|^2 + |\hat{H}_{n_r}(M-k)|^2) + \Gamma^{-1}} \\ W_{n_r,2}(k) = \frac{\hat{H}_{n_r}(k)}{\sum_{n_r=0}^{N_r-1} (|\hat{H}_{n_r}(k)|^2 + |\hat{H}_{n_r}(M-k)|^2) + \Gamma^{-1}} \end{cases}, \quad \text{for } k=0 \sim M-1 \text{ and } k \neq 0, M/2 \quad (12)$$

In Eqs. (11) and (12), $\Gamma = PT_s / N_0$ is the average signal-to-noise power ratio (SNR) and $[\cdot]^*$ denotes the complex conjugate operation.



(a) Without subcarrier combining



(b) With subcarrier combining

Fig. 4. Joint subcarrier combining and FDE with receive antenna diversity.

The demodulated frequency-domain signal $\{\tilde{S}(k); k=0 \sim M-1\}$ is then transformed back into the time-domain by M -point IDFT. After applying automatic gain control (AGC) [8] and picking out the real part, the demodulated time-domain signal $\{\tilde{s}(n); n=0 \sim M-1\}$ is given by

$$\begin{aligned} \tilde{s}(n) &= \frac{1}{\varepsilon} \text{Re} \left\{ \frac{1}{\sqrt{M}} \sum_{k=0}^{M-1} \tilde{S}(k) \exp\left(j2\pi n \frac{k}{M}\right) \right\} \\ &= s(n) + \text{Re} \{ \mu_{\text{ISI}}(n) + \mu_{\text{noise}}(n) \} \end{aligned} \quad (13)$$

where ε , $\mu_{\text{ISI}}(n)$, and $\mu_{\text{noise}}(n)$ are respectively the normalization factor of AGC, residual inter-sample interference and noise component.

Finally, the analog signal $\tilde{s}(t)$ is reconstructed by LPF from discrete-time sequence $\tilde{s}(n)$.

3. NMSE analysis

The NMSE for evaluating transmission performance is defined by

$$\text{NMSE} \equiv \frac{E[|\tilde{s}(n) - s(n)|^2]}{E[|s(n)|^2]} \quad (14)$$

Without loss of generality, the transmit signal is assumed to have unit average power. From Eq. (13), the NMSE becomes

$$\text{NMSE} = E[|\text{Re}\{\mu_{\text{ISI}}(n) + \mu_{\text{noise}}(n)\}|^2] \quad (15)$$

Since $\mu_{\text{ISI}}(n)$ and $\mu_{\text{noise}}(n)$ are real-valued and statistically independent, the variance $2\sigma^2$ of $\mu(n) = \mu_{\text{ISI}}(n) + \mu_{\text{noise}}(n)$ is expressed by

$$2\sigma^2 = E[|\mu(n)|^2] = E[|\text{Re}\{\mu(n)\}|^2] = 2\sigma_{\text{ISI}}^2 + 2\sigma_{\text{noise}}^2, \quad (16)$$

where $2\sigma_{\text{ISI}}^2$ and $2\sigma_{\text{noise}}^2$ are the variance of $\mu_{\text{ISI}}(n)$ and $\mu_{\text{noise}}(n)$, respectively. They are derived as (the derivation is omitted for the brevity)

$$\left\{ \begin{array}{l} 2\sigma_{\text{ISI}}^2 = \frac{\left| \frac{1}{M} \sum_{k=0}^{M-1} \sum_{n_r=0}^{N_r-1} \tilde{H}_{n_r}(k) \right|^2}{\left| \frac{1}{M} \sum_{k=0}^{M-1} \sum_{n_r=0}^{N_r-1} \tilde{H}_{n_r}(k) \right|^2} - 1 \\ 2\sigma_{\text{noise}}^2 = \frac{\frac{1}{\Gamma} \frac{1}{M} \sum_{k=0}^{M-1} \sum_{n_r=0}^{N_r-1} |\tilde{W}_{n_r}(k)|^2}{\left| \frac{1}{M} \sum_{k=0}^{M-1} \sum_{n_r=0}^{N_r-1} \tilde{H}_{n_r}(k) \right|^2} \end{array} \right. \quad (17)$$

where $\tilde{H}_{n_r}(k)$ and $\tilde{W}_{n_r}(k)$ is given by

$$\tilde{H}_{n_r}(k) = \begin{cases} W_{n_r}(k) \hat{H}_{n_r}(k) & , k=0, M/2 \\ W_{n_r,1}(k) \hat{H}_{n_r}(k) + W_{n_r,2}(M-k) \hat{H}_{n_r}^*(M-k) & , \text{otherwise} \end{cases} \quad (18)$$

$$|\tilde{W}_{n_r}(k)|^2 = \begin{cases} |W_{n_r}(k)|^2 & , k=0, M/2 \\ |W_{n_r,1}(k)|^2 + |W_{n_r,2}(M-k)|^2 & , \text{otherwise} \end{cases} \quad (19)$$

The conditional NMSE for given set of channel gains $\{H_{n_r}(k); k=0 \sim M-1, n_r=0 \sim N_r-1\}$ can be calculated from Eqs. (15)~(17) as

$$\begin{aligned} \text{NMSE}(\Gamma, \{H_{n_r}(k)\}) &= 2\sigma_{\text{ISI}}^2 + 2\sigma_{\text{noise}}^2 \\ &= \frac{\frac{1}{M} \sum_{k=0}^{M-1} \left| \sum_{n_r=0}^{N_r-1} \tilde{H}_{n_r}(k) \right|^2 + \frac{1}{\Gamma} \frac{1}{M} \sum_{k=0}^{M-1} \sum_{n_r=0}^{N_r-1} |\tilde{W}_{n_r}(k)|^2}{\left| \frac{1}{M} \sum_{k=0}^{M-1} \sum_{n_r=0}^{N_r-1} \tilde{H}_{n_r}(k) \right|^2} - 1. \end{aligned} \quad (20)$$

Table 1. Numerical evaluation/Computer simulation condition.

Signal transmission	Analog SC-FDE with Subcarrier Combining
Analog signal	Voice (short news)
Sampling rate	1/T=8 kHz
DFT size	M=64
Spectrum shaping filter	Ideal brick wall LPF
Mapping	Distributed mode
Total no. of subcarriers	$N_c=8192$
CP length	$N_g=16$
No. of Tx antennas	$N_t=1$
No. of Rx antennas	$N_r=1 \sim 4$
Channel	Frequency-selective block Rayleigh fading
	L=16-path exponential power delay profile with decay factor $\beta=0, 3, 6\text{dB}$
FDE weight	MMSE
Channel estimation & Fast AGC	Ideal

The denominator of the first term in Eq. (20) expresses the power coefficient of desired signal. From Eqs. (12), (18) and (20), it should be noted that the power coefficient of desired signal is composed of the sum of $|\hat{H}_{n_r}(k)|^2$ and $|\hat{H}_{n_r}(M-k)|^2$ for $n_r=0 \sim N_r-1, k=0 \sim M-1$ except $k=0, M/2$. In other words, subcarrier combining achieves an antenna diversity order of approximately $2 \times N_r$. However, the achievable diversity order depends on correlation between $|\hat{H}_{n_r}(k)|^2$ and $|\hat{H}_{n_r}(M-k)|^2$ (i.e., channel frequency-selectivity strength) indeed. This is also discussed in simulation results.

The average NMSE can be numerically evaluated by averaging Eq. (20) over all possible realizations of $\{H_{n_r}(k); k=0 \sim M-1, n_r=0 \sim N_r-1\}$.

4. Numerical Evaluation and Computer Simulation Results

4.1. Numerical and Computer Simulation Condition

The conditions for the numerical evaluation of theoretical average NMSE and computer simulation are summarized in Table 1. We assume the bandwidth-limited (4 kHz) voice transmission (a news announcer voice). A sampling rate of 1/T=8 kHz (sample duration of T=0.125 msec), a time-domain signal block of M=64 samples, an adjacent subcarrier interval of 125 Hz, and a distributed mapping over $N_c=8192$ subcarriers are also assumed. As a propagation channel, Rayleigh fading channel having a T_s -spaced ($T_s=T \times M/N_c \approx 1\mu\text{sec}$) L=16-path with exponential power delay profile, where β is decay factor, is considered. A very slow (or block) fading model is assumed, where fading stays unchanged over each block of $N_c=8192$ samples for analog SC-FDE. The time delay of l-th path is set to $\tau_{n_r,l}=l$ and the maximum delay difference is less than CP length. Ideal channel estimation and ideal fast AGC are also assumed.

The numerical evaluation of theoretical average NMSE is done by Monte-Carlo numerical computation method as follows. The set of path gains $\{h_{n_r,l}; l=0 \sim L-1\}$ is generated for obtaining channel gain and MMSE-FDE weight using Eqs. (8), (11) and (12). This is repeated sufficiently to obtain the average NMSE.

4.2. NMSE Performance

The NMSE performance of analog SC-FDE with subcarrier combining is shown in Fig. 5. For comparison, the performance without subcarrier combining is also plotted. A fairly good agreement between the numerical and simulation results is found. It is obvious that the NMSE performance of analog SC-FDE with subcarrier combining is improved owing to the additional frequency diversity gain. By exploiting the complex conjugate

relation between the LSB and USB subcarriers, subcarrier combining with N_r receive antennas can achieve similar diversity order to $(2 \times N_r)$ -branch receive antenna diversity. However, a performance degradation of approximately 3 dB is seen in comparison of subcarrier combining having N_r receive antennas and the case having $2 \times N_r$ receive antennas without subcarrier combining. The reason is discussed as follows. At the receiver, two subcarriers having complex conjugate relation in desired signal are used for subcarrier combining to reproduce two frequency components. Therefore, the demodulated frequency components also have the complex conjugate relation, thereby producing the complex conjugate relation between LSB and USB of the recovered analog signal. In other words, the impact of inter-sample interference and noise becomes double those in analog SC-FDE without subcarrier combining. This leads to the performance degradation. As N_r increases, the space diversity gain becomes the dominant factor of performance improvement. Therefore, the effect of subcarrier combining, which leads to the performance improvement, visibly becomes smaller as shown in Fig. 5.

Fig. 6 shows comparison between the effect of subcarrier combining and space-time transmit diversity (STTD) [9] on analog SC-FDE. In case of using STTD, the number N_t of transmit antennas was set to $N_t=2$. It is easily confirmed that subcarrier combining achieves similar diversity order to 2-branch transmit antenna diversity. A minor difference is seen because the subcarrier $\tilde{R}(k)$ at $k=0, M/2$ cannot obtain additional frequency diversity gain by subcarrier combining as the others.

The additional diversity gain obtained by subcarrier combining depends on the strength of channel frequency-selectivity. Investigation results of this impact on NMSE performance are shown in Figs. 7 and 8. Fig. 7 shows the NMSE performance in case of decay factor $\beta=0, 3, 6$ dB. As β increases, the channel frequency-selectivity becomes weaker, thereby degrading the NMSE performance due to a smaller diversity gain. It is confirmed that $\beta=0$ (a uniform power delay profile) gives the best performance. On the other hand, Fig. 8 plots the NMSE performance as a function of normalized root mean square (rms) delay spread τ_{rms}/T_s . It is seen that as $\tau_{rms}/T_s > 0.5$ (corresponding to the number of paths $L > 2$ for $\beta=0$ dB and $L > 3$ for $\beta=6$ dB), additional frequency diversity gain by subcarrier combining is sufficiently obtained. Fig. 8 also confirmed that the case of $\beta=0$ dB (a strong frequency-selective channel) gives the better performance than the case of $\beta=6$ dB (a weak frequency-selective channel).

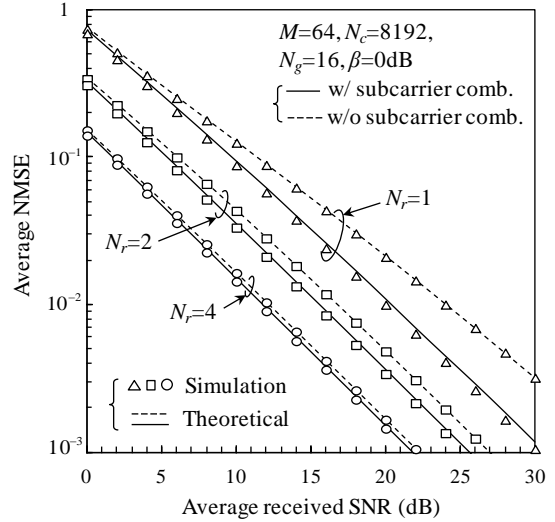


Fig. 5. NMSE performance.

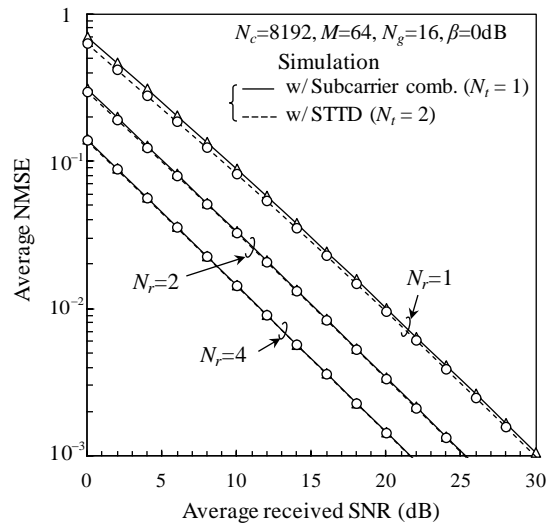


Fig. 6. Comparison between subcarrier combining and STTD.

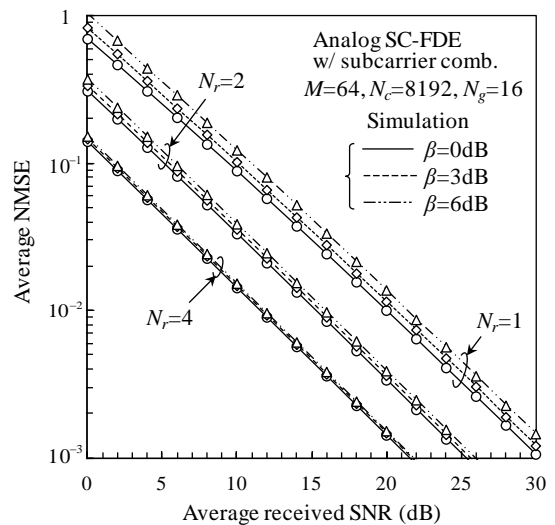


Fig. 7. Impact of decay factor β on NMSE performance.

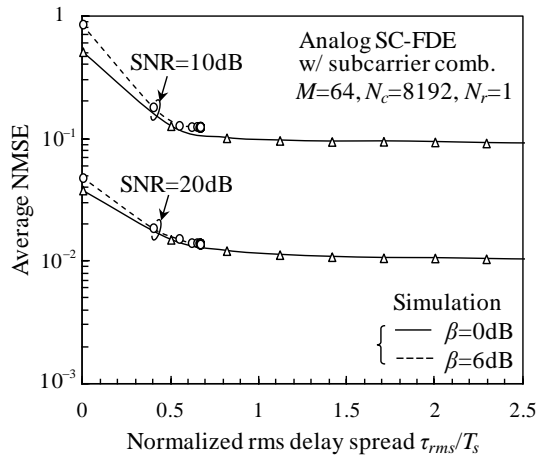


Fig. 8. Impact of channel frequency-selectivity on NMSE performance.

5. Conclusion

In this paper, by exploiting the complex conjugate relation between the LSB and USB subcarriers of a real-valued signal, a subcarrier combining method for analog SC-FDE is proposed in order to further improve the NMSE performance. A theoretical analysis of the NMSE performance was presented and confirmed by computer simulation. It was shown that subcarrier combining can improve the NMSE performance and achieve similar diversity order to 2-branch antenna diversity. The impact of channel frequency-selectivity on NMSE performance was also investigated to show the effectiveness of

subcarrier combining.

References

- [1] Y. Kim, B. J. Jeong, J. Chung, C.-S. Hwang, J. S. Ryu, K.-H. Kim, and Y. J. Kim, "Beyond 3G; vision, requirements, and enabling technologies," *IEEE Commun. Mag.*, vol.41, no.3, pp.120-124, March 2003.
- [2] Y. Park and F. Adachi, *Enhanced radio access technologies for next generation mobile communication*, Springer, 2007.
- [3] A. Goldsmith, *Wireless communications*, Cambridge University Press, 2005.
- [4] T. H. Vo, S. Kumagai, T. Obara, and F. Adachi, "Analog single-carrier transmission with frequency-domain equalization," *IEICE Trans. Commun.*, vol.E97-B, no.9, pp.1958-1966, Sept. 2014.
- [5] D. Falconer, S. L. Ariyavistakul, A. Benyamin-Seeyar, and B. Eidson, "Frequency domain equalization for single-carrier broadband wireless systems," *IEEE Commun. Mag.*, vol.40, no.4, pp.58-66, April 2002.
- [6] F. Adachi, H. Tomeba, and K. Takeda, "Frequency-domain equalization for broadband single-carrier multiple access," *IEICE Trans. Commun.*, vol.E92-B, no.5, pp.1441-1456, May 2009.
- [7] H. G. Myung, J. Lim, and D. J. Goodman, "Single carrier FDMA for uplink wireless transmission," *IEEE Vehicular Technol. Mag.*, vol.1, no.3, pp.30-38, Sept. 2006.
- [8] Y. Han, Z. Wang, L. Li, and Y. Zhao, "A fast automatic gain control scheme for IEEE 802.15.4 receiver," *Proc. IET 2nd International Conference on Wireless, Mobile and Multimedia Networks (ICWMMN)*, pp.167-170, Oct. 2008.
- [9] T. H. Vo, S. Kumagai, and F. Adachi, "A novel analog signal transmission using joint space-time transmit diversity and receive antenna diversity," *Proc. IEEE 80th Vehicular Technology Conference (VTC2014-Fall)*, Sept. 2014.